ANALYSIS OF VISUAL ESTIMATION OF SYSTEM STATE FROM ARBITRARY DISPLAYS

Patrick A. Gainer
Langley Research Center

SUMMARY

A method is presented for implementing the state estimator of the manual control model when the system output is a visual display of arbitrary form; that is, the display may be pictorial, including real world, or made up of dials and pointers. The method is used to provide error criteria for a lookpoint controller that appears to be capable of modeling human scanning behavior. This model, if combined with a model of the control process, should be useful in predicting effects of changes in displays on performance of flight tasks.

INTRODUCTION

One of the most important elements of a model of manual control is some form of state estimator. This element receives system outputs and converts them into an estimate of the system state in a form suitable for input to a control algorithm.

The state estimator is usually modelled as a Kalman estimator, which minimizes the variance of the estimated state, and which is capable of accepting sampled data. The output of the estimator includes an estimate of the covariance of the state estimate. This covariance depends on the probable errors in the data, and not on the data. In many cases, such an estimate of covariance is sufficient for an analysis of system performance by the use of covariance propagation techniques. Furthermore, when covariance can be estimated prior to actual data input, an optimum sequence of samples can be predetermined.

Due to the nature of the visual sense, human observers are usually forced to scan a scene in a series of lookpoints in order to extract its information content. If the scene is changing, each lookpoint constitutes a sample of output data of a dynamic system. All that is required for applying the Kalman estimator as a model of human visual observation is a means of estimating probable errors of observation at any lookpoint.

This paper presents a means of estimating the errors to be expected when a human observer estimates the state of a system by looking at a display of some set of system outputs. The display may be pictorial, including "real world," or made up of discrete dials, pointers, etc.

First, the method of estimating the covariance of the state estimate at a given lookpoint will be described. Then the means, and some results, of devising a lookpoint controller to simulate human scanning behavior will be discussed. This latter work is presented in full detail in reference 1.

SYMBOLS

x	state vector
$\hat{x}$	estimated state vector
y	output vector
$[C]$	matrix of coefficients relating state and output vectors
V	standard error of observation of output
$[C]^T$	transpose of C
$[\mathrm{cov}(y)]$	covariance matrix of output vector
$[\mathrm{cov}(x)]$	covariance matrix of estimated state vector
θ	pitch angle
ϕ	roll angle
ψ	yaw angle

Abbreviation:

VSI	Vertical Speed Indicator
GSI	Glide Slope Indicator

A dot over a variable denotes a derivative with respect to time.

METHOD OF ANALYSIS

Figure 1 is a manual control block diagram that is borrowed from reference 2. The state estimator in figure 1 will be considered to have in it some means of solving the relationship:

$$y(t) = C\,x(t) + V(t) \tag{1}$$

where $x(t)$ is system state vector
C is a matrix of constant sensitivities

$y(t)$ is visible system output vector
$V(t)$ is random error vector

The sources of error $V(t)$ are in the display and measurements $V_m(t)$ and in the visual sensing of the pilot $V_d(t)$.

$$V(t) = V_m(t) + V_d(t)$$

The visual errors V_d are the ones that vary with lookpoint. Thus, figure 1 may be considered to represent the pilot model at a fixed lookpoint. At a different lookpoint, V_d, and therefore y and $\hat{x}$, may be different.

The perceived system output $y(t)$, which is the input to the state estimation process, might be specified in several ways. For example, in a display composed of discrete instruments, one of the elements of $y(t)$ might be taken to be the altitude, since that quantity is displayed by the altimeter. A more general approach that allows treatment of pictorial as well as discrete displays is to take as elements of $y(t)$ the displacement, rate of change of displacement, and rate of change of displacement of points in the display (e.g., points on the altimeter needle). Consider the display to be broken into segments. The portion of the display in each segment is rigid so that one point in a segment may be taken to represent the whole segment. Rotating display elements should be represented by more than one segment, so that rotation of any one segment can be neglected. This point may be seen to move vertically or horizontally or both in response to one or more of the state variables $x(t)$. Taking each component as a separate indicator of system output, each point in the display may provide four elements of $y(t)$: vertical and horizontal displacement and vertical and horizontal rate of change of displacement from a nominal position.

The next step is to perturb each state variable in turn and to calculate the resulting effects on each display segment. These effects will be expressed as linear influence coefficients which are, either exactly or approximately, partial derivatives of vertical and horizontal angular displacement and rate of displacement, as measured at the observer's eye, with respect to the system state variables. These influence coefficients are, of course, the elements of the matrix C in equation 1.

The random error $V(t)$ remains to be specified. That part of it that is due to the visual sense $V_d(t)$ depends on the observer's acuity at each display point, which in turn depends on the location of the display point with respect to the observer's lookpoint. From a knowledge of the observer's resolving power at any point in his visual field and of where he is looking, one can estimate the element of $V(t)$ for each display segment. Typical resolution curves are shown in figures 2 and 3. For any given lookpoint, the eccentricity angle (visual angle between lookpoint and display point) of each display point is calculated, and the corresponding resolutions from figures 2 and 3 are taken as standard deviations for calculating $V_d(t)$.

Now the minimum variance estimate of $x(t)$ may be formulated from equation 1. This estimate is:

$$\hat{x}(t) = \left[C^T [cov(y)]^{-1} C\right]^{-1} C^T [cov(y)]^{-1} y(t) \qquad (2)$$

The matrix $cov(y)$ is the covariance of $y(t)$ which, for the case of uncorrelated measurement errors, is a diagonal matrix formed by squaring the elements of $V(t)$. If measurement errors are known to be correlated, there will of course be off-diagonal terms in $cov(y)$, but equation 2 is still valid. What is required in this paper, as well as $\hat{x}(t)$, is an estimate of its covariance. It may be shown (ref. 3) that the covariance of $x(t)$ is:

$$cov(\hat{x}) = \left[C^T [cov(y)]^{-1} C\right]^{-1} \qquad (3)$$

It is seen that, since for each different lookpoint there is a different matrix $[Cov(y)]$, the covariance of the estimated state varies with lookpoint.

Example

In order to demonstrate how to calculate $cov(x)$ for a given lookpoint, a simple example has been concocted. Two hypothetical displays will be compared for each of two lookpoints.

Figure 4 shows two displays, each of which is capable of showing three variables. When all three variables are at zero, both displays look the same. In Display A all three line segments move together as in figure 4(b). In Display B, each segment responds to a different variable, as in figure 4(c). Suppose that the variables presented are pitch, roll and yaw angles, and let the display be viewed from such a distance that movement of 1 degree visual angle represents 1 degree pitch or yaw (according to direction), and 1 degree rotation of the display in its plane represents 1 degree of roll.

The displays are of such size that each line segment subtend 11 degrees of visual angle.

The display area must be divided into discrete areas, a point in each area being taken as the indicator of system output for that area as shown in figure 5. Sensitivities of these points to changes in state variables are calculated in terms of change of visual angle or angular rate per unit change in each state variable. These calculated sensitivities are given in table I. The sensitivity matrix [C] would have in the general case four rows for each segment. For the illustrative cases in this paper, certain movements were considered negligible or not visible. The sensitivities of these movements, being zero, were omitted from the table to save space. For example, horizontal movement, due to rotation, of a point on a horizontal line was neglected. Also, motion along a line was considered not visible. If the lines were really

made up of dots, this motion could be seen, and the sensitivity matrix would have corresponding terms. Segment 6 is, in fact, the only one in which both vertical and horizontal components of motion were considered to be visible, and so it appears four times in table I for each display.

The accuracy of observation depends on the observer's acuity and his lookpoint. In order to simplify estimation of parafoveal acuity, it is assumed that contours of constant acuity are circles centered on the lookpoint. This assumption is not essential to the method, but the spread of available acuity data is great enough that a more detailed mapping seems unwarranted.

Two lookpoints were chosen for illustrating the method: one at the intersection of the lines, and one 6 degrees to the right of the intersection, on the horizontal line. For each lookpoint, eccentricities were calculated for the points in the display for which sensitivities were calculated. For these eccentricities, resolutions were read from the curves. The resolutions were used as the elements of $[\mathrm{cov}(y)]$.

The covariance matrices of the estimated state $\mathrm{cov}(x)$ were computed from equation 3 and presented in tables II and III. Table II is for Display A. Note the way correlation between pitch, roll, and yaw, as shown by the off-diagonal terms, changes with lookpoint. There is no correlation between displacement and rate for either lookpoint.

The covariances for Display B are diagonal matrices for both lookpoints.

As might be expected, the variance of estimate of any given state variable depends on lookpoint. This dependence on lookpoint is much less for those variables that are perceived through sensation of rate, as rate resolution varies much less across the field of vision than does position resolution.

Scanning Behavior

If the display elements did not move while the observer looked around, the covariance of $x(t)$ could be reduced by combining directly the information from several lookpoints. This reduction would be easy to estimate. However, since $\hat{x}(t)$ represents the state of a dynamic system, the observer, in trying to improve his estimate of any state variable by attending to another point in the display, finds that the uncertainty of the information he obtained from the first point increases while he looks at the second. The optimum means of combining sequential observations of a dynamic system is the Kalman estimator. This estimation algorithm also provides a method for deciding which one of a number of possible observations it would be best to make, provided that the probable error of each possible observation is known beforehand. Combining the Kalman estimator with the method of this paper, for estimating the covariance matrix of the output, $\mathrm{cov}(y)$, one may devise a lookpoint controller, as has been done in reference 1, from which the following material is taken.

Figure 6 shows the information flow for this controller, which has been applied to the instrument array shown in figure 7. Figure 8 shows what happens to the variances when the lookpoint is arbitrarily forced to follow the time history in the figure. For these results, the system state transition matrix that governs the growth of covariance is taken to be that of a second order dynamic system without damping or cross-coupling.

In order for the lookpoint controller to choose its own lookpoint, it must have some strategy. Figure 9 illustrates what happens when the lookpoint is chosen so as to provide information about the state variable with the greatest weighted variance. (It is necessary to weight the variances because of dimensionality of each state variable and its importance in control of the system.) Figure 9 represents a case of an autopilot-controlled ("coupled") landing approach where the command bars in the flight director are inactive. Figure 10 is the computed time history of lookpoints over 6.5 seconds, when the GSI and artificial horizon are combined into a single lookpoint identified as Flight Director.

A manually controlled landing approach was simulated simply by adding command bars as variables that need attention. The same lookpoint selection strategy was used, with results as shown in figure 11 when command bars are included along with GSI and artificial horizon in the Flight Director.

In spite of the many simplifying assumptions, the time histories in figures 10 and 11 are quite "Humanoid." The flight director gets most of the attention, and it gets more attention in manual control than in monitoring the autopilot (68 percent of total time compared to 57 percent in monitoring). During monitoring, transitions between peripheral instruments are more likely to happen than during manual control, where nearly all transitions are between flight director and peripheral instruments. However, because of the assumptions and especially because a number of instruments were omitted (Horizontal Situation Indicator, for example), there is no direct comparison with available eye movement data.

CONCLUDING REMARKS

A method has been presented for implementing the state estimator of the manual control model when the system output is a visual display of arbitrary form; that is, the display may be pictorial, including real world, or made up of dials and pointers. The method has been used to provide error criteria for a lookpoint controller that appears to be capable of modeling human scanning behavior. This model, if combined with a model of the control process, should be useful in predicting effects of changes in displays on performance of flight tasks.

REFERENCES

1. Mout, Michael L., Burgin, George H., and Walsh, Michael J.: Use of Sensitivity Analysis to Predict Pilot Performance as a Function of Different Displays. NASA CR 2906, November 1977.

2. Karmarker, J, S., and Sorensen, J. A.: Information and Display Requirements for Independent Landing Monitors. NASA CR 2687, August 1976.

3. Gainer, Patrick A.: A Method for Computing the Effect of an Additional Observation on a Previous Least Squares Estimate. NASA TN D-1599, January 1963.

TABLE I.- SENSITIVITY COEFFICIENTS

(a) Display A

Segment	State Variable: θ	ϕ	ψ	$\dot{\theta}$	$\dot{\phi}$	$\dot{\psi}$
1	1	-.1738	0	0	0	0
2	1	-.1391	0	0	0	0
3	1	-.1045	0	0	0	0
4	1	-.070	0	0	0	0
5	1	-.035	0	0	0	0
6	1	0	0	0	0	0
6	0	0	1	0	0	0
7	0	.035	0	0	0	0
8	0	.070	0	0	0	0
9	0	.1045	0	0	0	0
10	0	.1391	0	0	0	0
11	0	.1738	0	0	0	0
12	0	.035	1	0	0	0
13	0	.070	1	0	0	0
14	0	.1045	1	0	0	0
15	0	.1391	1	0	0	0
16	0	.1738	1	0	0	0
1	0	0	0	1	-.1738	0
2	0	0	0	1	-.1391	0
3	0	0	0	1	-.1045	0
4	0	0	0	1	-.070	0
5	0	0	0	1	-.035	0
6	0	0	0	1	0	0
6	0	0	0	0	0	1
7	0	0	0	0	.035	0
8	0	0	0	0	.070	0
9	0	0	0	0	.1045	0
10	0	0	0	0	.1391	0
11	0	0	0	0	.1738	0
12	0	0	0	0	.035	1
13	0	0	0	0	.070	1
14	0	0	0	0	.1045	1
15	0	0	0	0	.1391	1
16	0	0	0	0	.1738	1

TABLE I.- Concluded

(b) Display B

Segment	State Variable: θ	ϕ	ψ	$\dot{\theta}$	$\dot{\phi}$	$\dot{\psi}$
1	1	0	0	0	0	0
2	1	0	0	0	0	0
3	1	0	0	0	0	0
4	1	0	0	0	0	0
5	1	0	0	0	0	0
6	1	0	0	0	0	0
6	0	0	1	0	0	0
7	0	.035	0	0	0	0
8	0	.070	0	0	0	0
9	0	.1045	0	0	0	0
10	0	.1391	0	0	0	0
11	0	.1738	0	0	0	0
12	0	0	1	0	0	0
13	0	0	1	0	0	0
14	0	0	1	0	0	0
15	0	0	1	0	0	0
16	0	0	1	0	0	0
1	0	0	0	1	0	0
2	0	0	0	1	0	0
3	0	0	0	1	0	0
4	0	0	0	1	0	0
5	0	0	0	1	0	0
6	0	0	0	1	0	0
6	0	0	0	0	0	1
7	0	0	0	0	.035	0
8	0	0	0	0	.070	0
9	0	0	0	0	.1045	0
10	0	0	0	0	.1391	0
11	0	0	0	0	.1738	0
12	0	0	0	0	0	1
13	0	0	0	0	0	1
14	0	0	0	0	0	1
15	0	0	0	0	0	1
16	0	0	0	0	0	1

TABLE II.- DISPLAY A COVARIANCES

[Units are (arc min)^2 and (arc min/sec)^2]

Lookpoint at Intersection

θ	$\dot{\theta}$	ϕ	$\dot{\phi}$	ψ	$\dot{\psi}$
.404	0	0	0	0	0
0	488	0	0	0	0
0	0	130	0	-1.66	0
0	0	0	39080	0	-3970
0	0	-1.66	0	.496	0
0	0	0	-3970	0	1489

Lookpoint at 6° to Right of Intersection

1.146	0	-11.41	0	.824	0
0	508	0	-403	0	34.1
-11.41	0	178	0	-12.8	0
0	-403	0	37146	0	-3143
.824	0	-12.8	0	5.48	0
0	34.1	0	-3143	0	1218

TABLE III.- DISPLAY B COVARIANCES

[Units are $(\text{arc min})^2$ and $(\text{arc min/sec})^2$]

Lookpoint at Intersection

θ	$\dot{\theta}$	ϕ	$\dot{\phi}$	ψ	$\dot{\psi}$
.475	0	0	0	0	0
0	886	0	0	0	0
0	0	374	0	0	0
0	0	0	85561	0	0
0	0	0	0	.475	0
0	0	0	0	0	886

Lookpoint at 6° to Right of Intersection

5.98	0	0	0	0	0
0	1006	0	0	0	0
0	0	38.8	0	0	0
0	0	0	75960	0	0
0	0	0	0	4.56	0
0	0	0	0	0	952

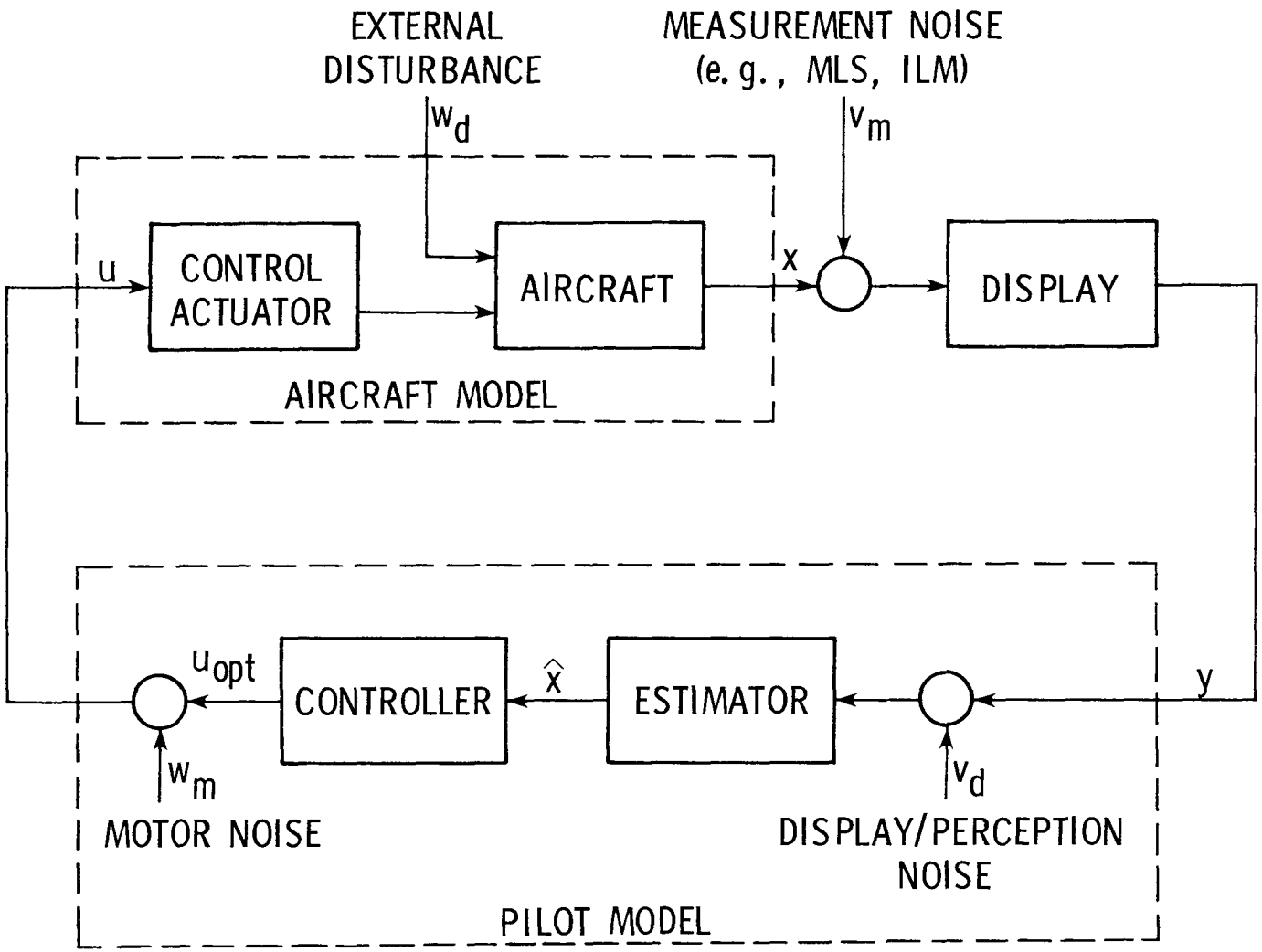

Figure 1.- Manual control system block diagram.

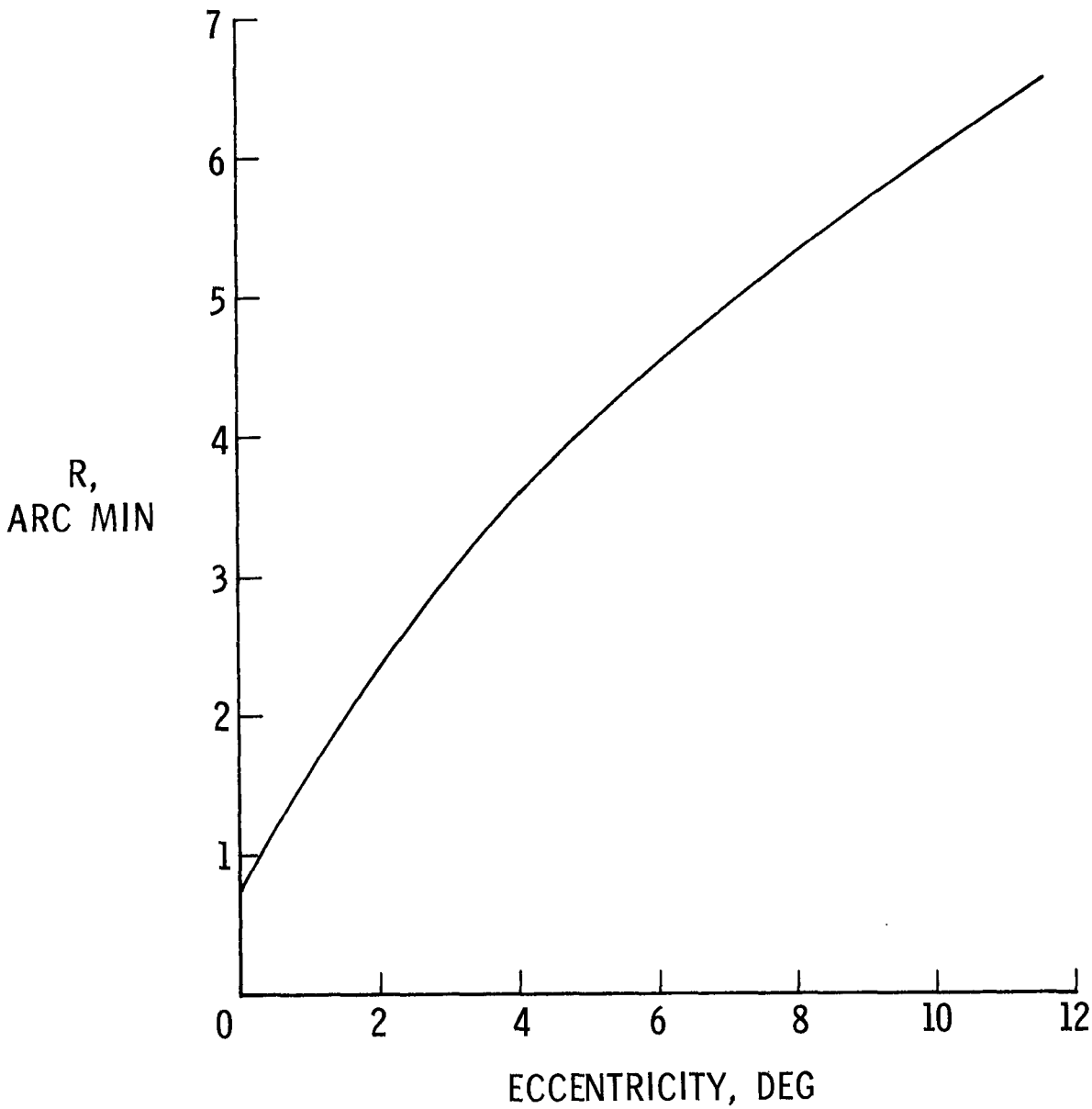

Figure 2.- Displacement resolution versus foveal eccentricity.

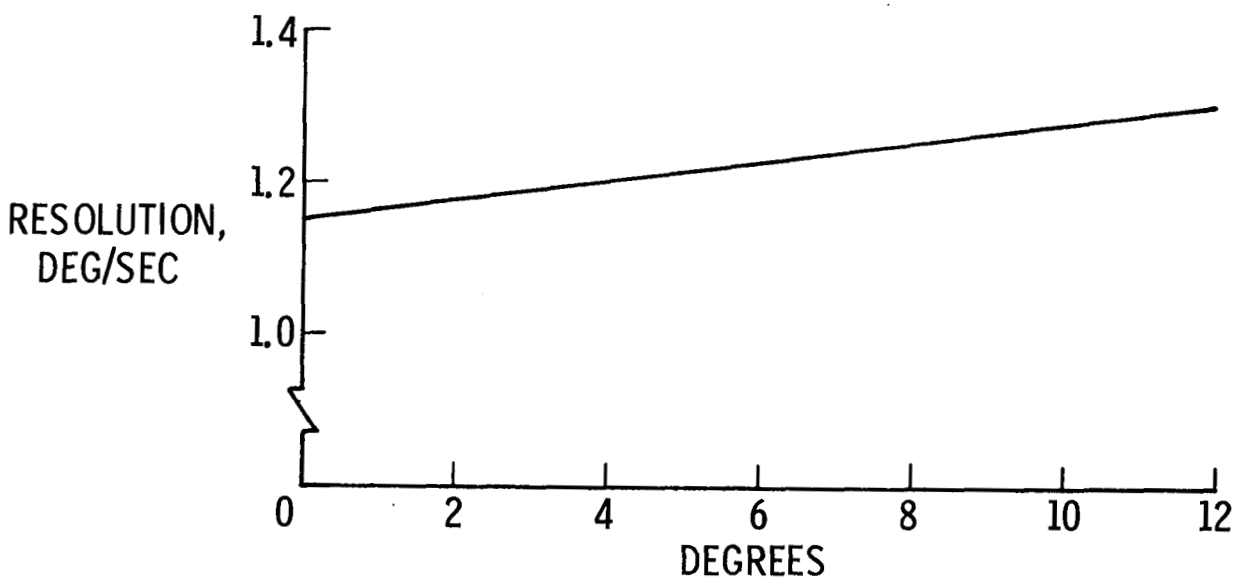

Figure 3.- Rate resolution versus foveal eccentricity.

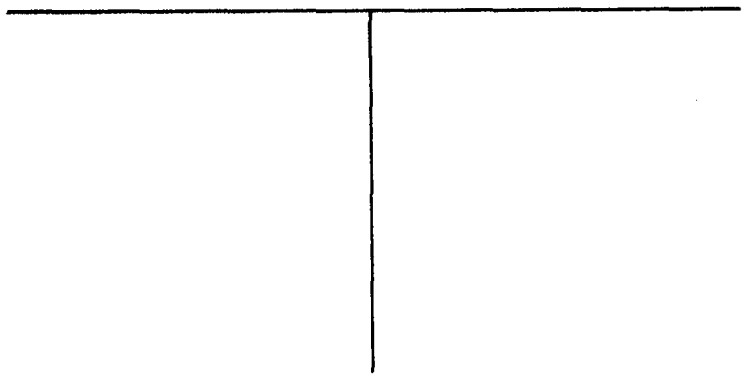

(a) Display formats A and B at rest.

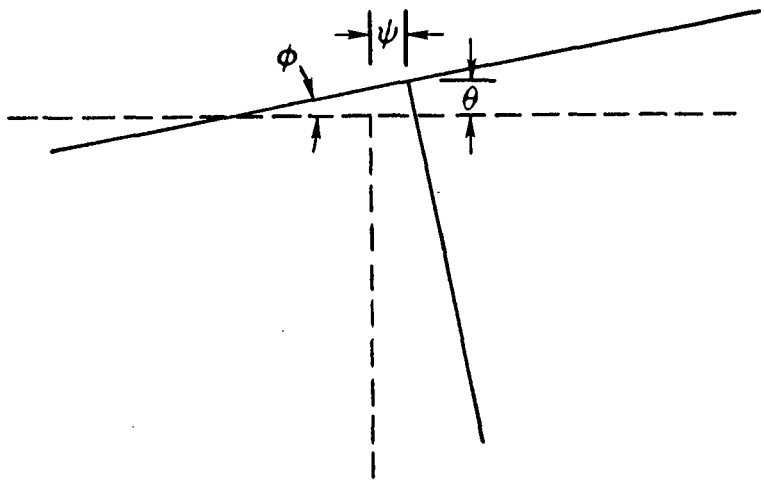

(b) Display A deflected in pitch, roll, and yaw.

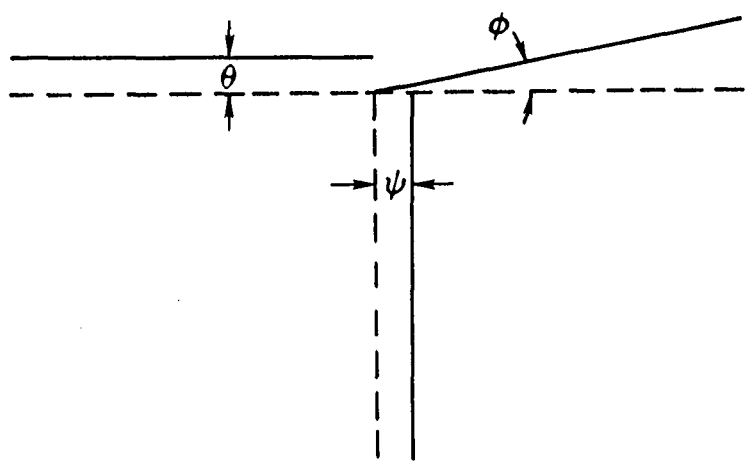

(c) Display B deflected in pitch, roll, and yaw.

Figure 4.- Fictitious displays used in illustrative example.

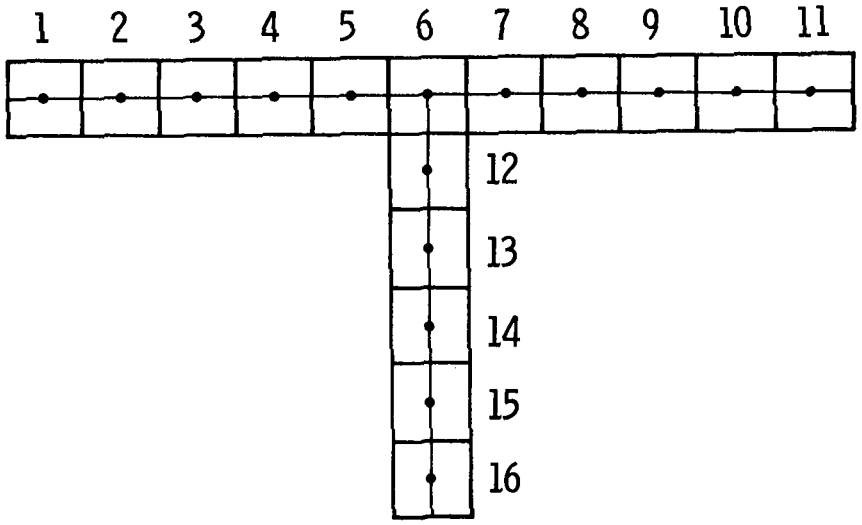

Figure 5.- Display segments.

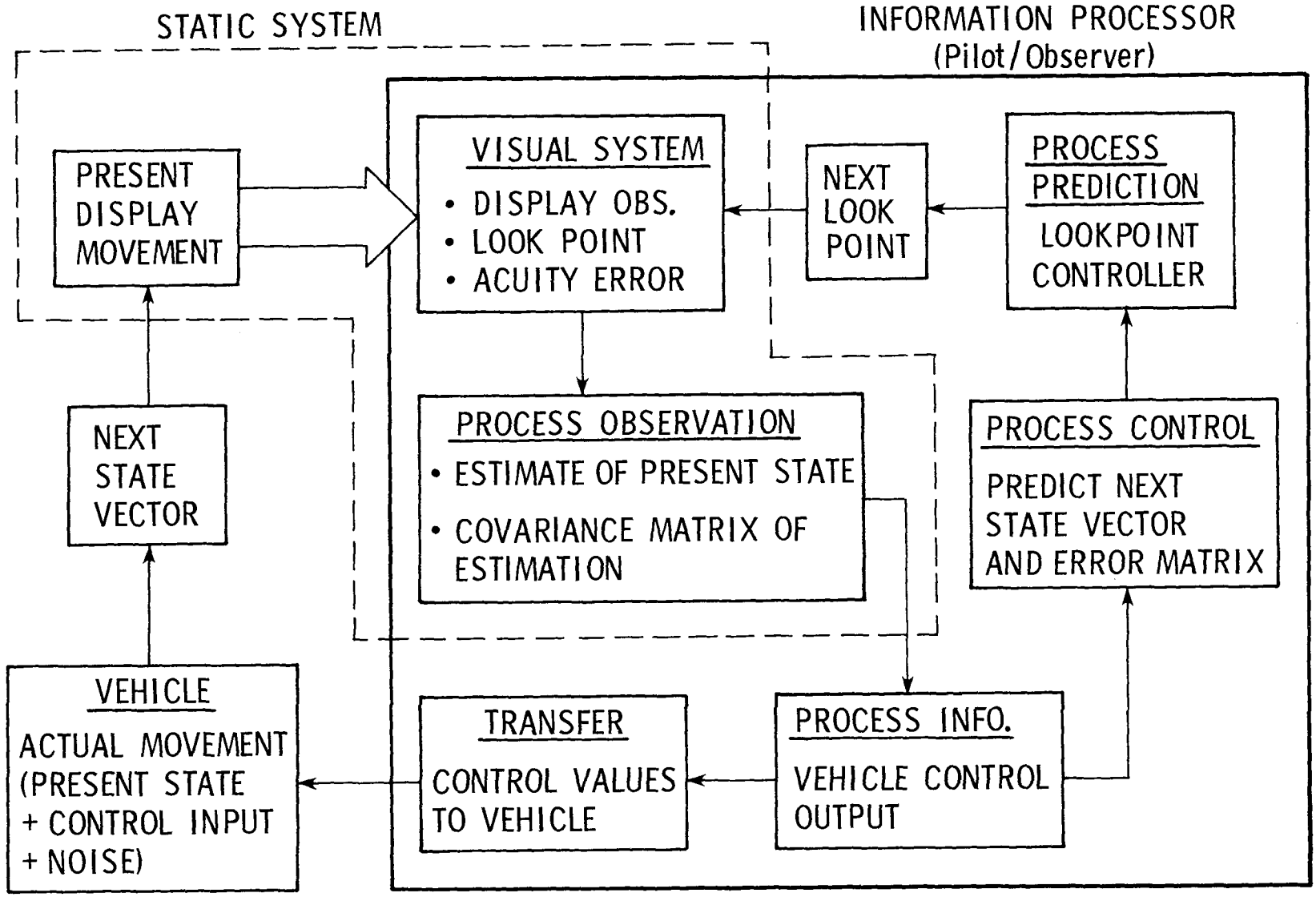

Figure 6.- Information flow for dynamic system.

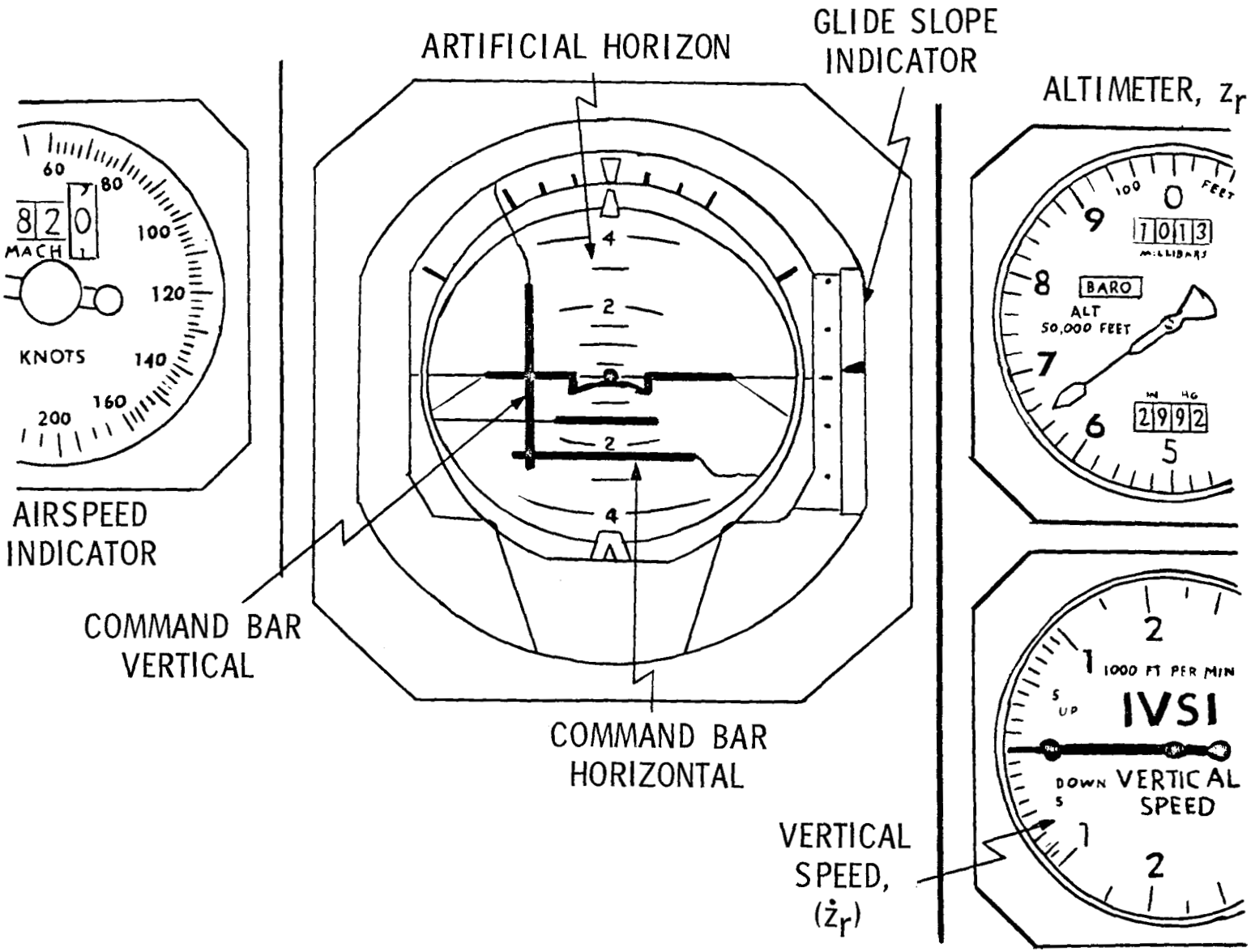

Figure 7.- Display setup.

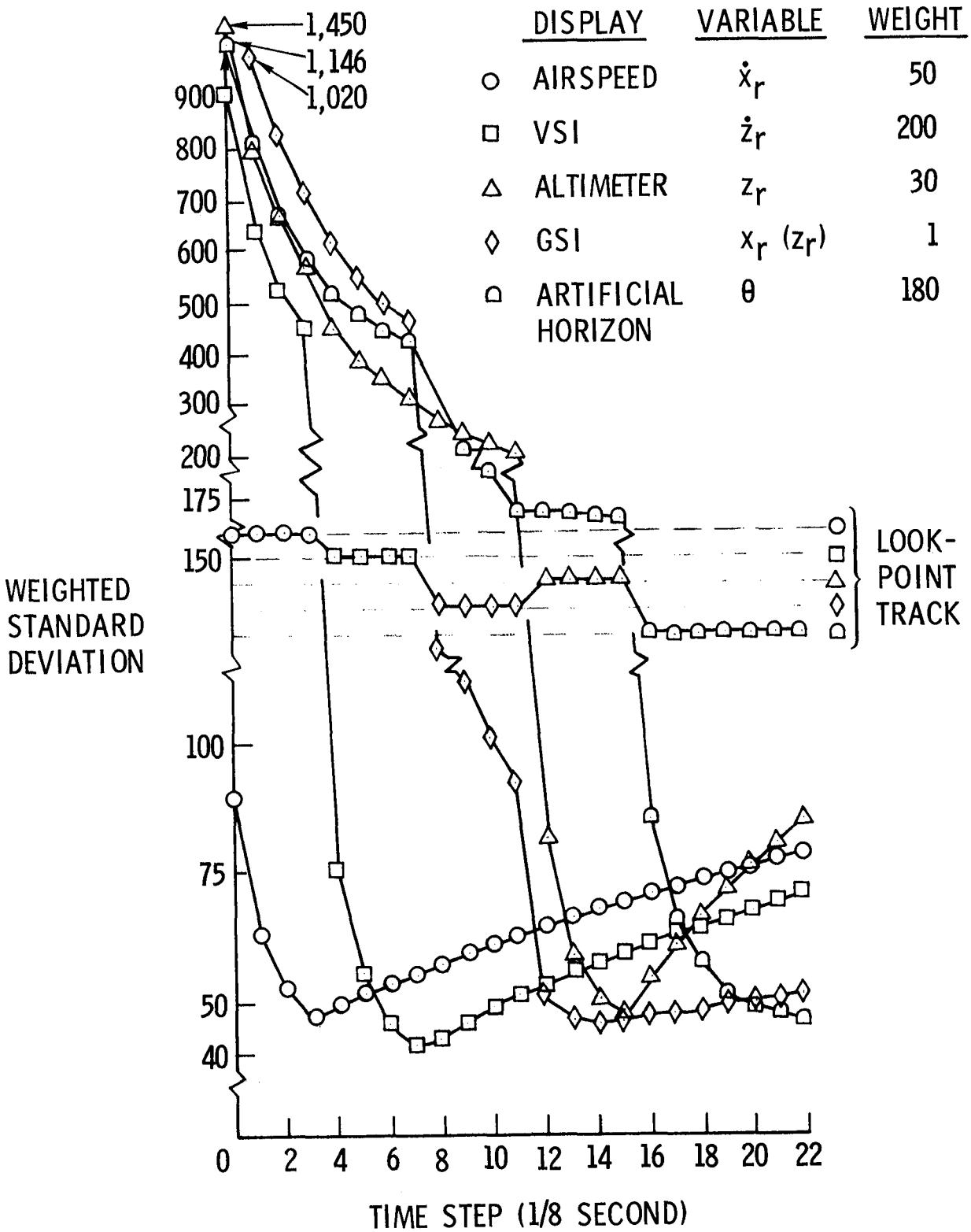

Figure 8.- Fixed lookpoints.

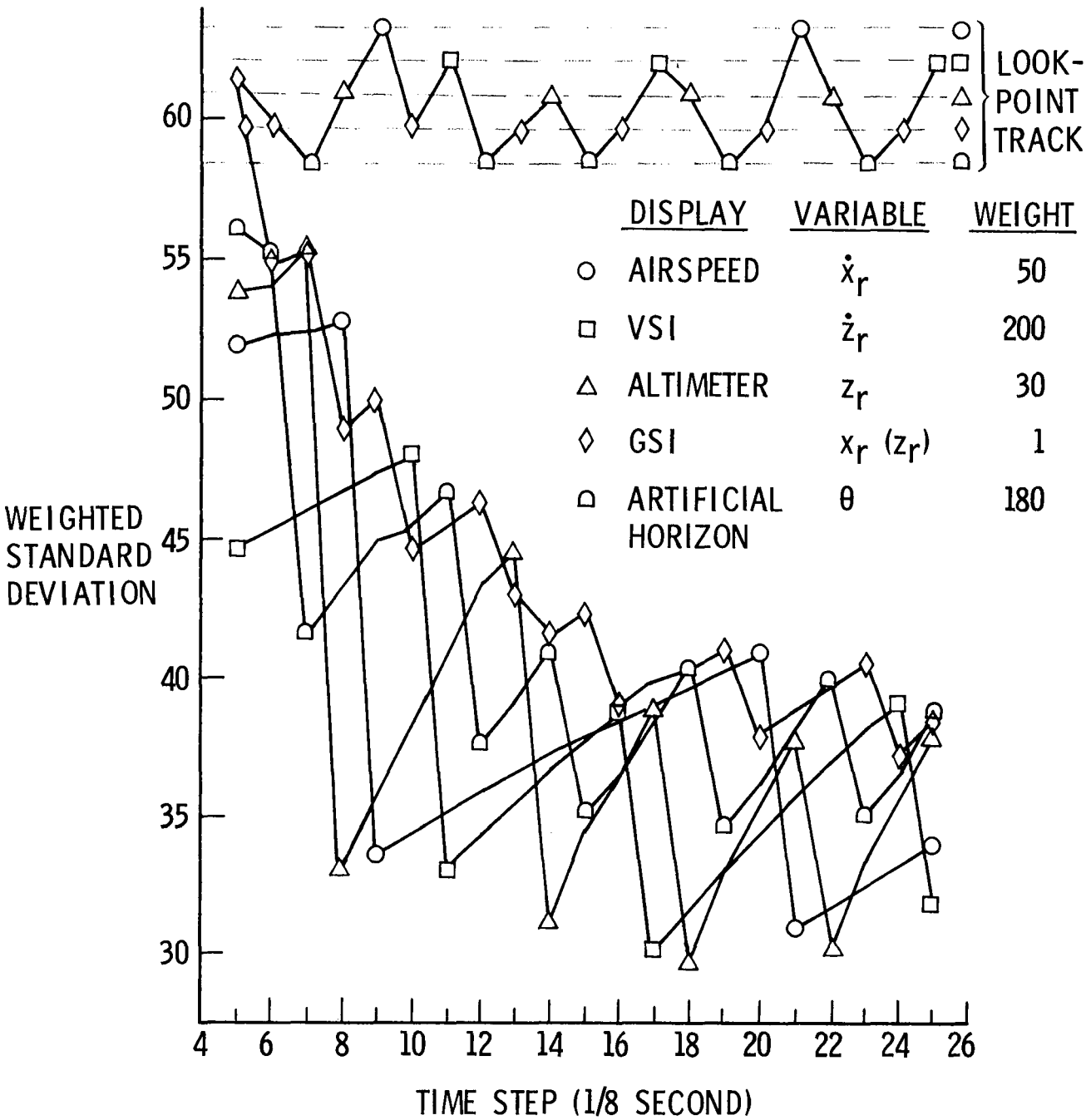

Figure 9.- Lookpoint controller minimizing maximum weighted variance in automatic landing approach.

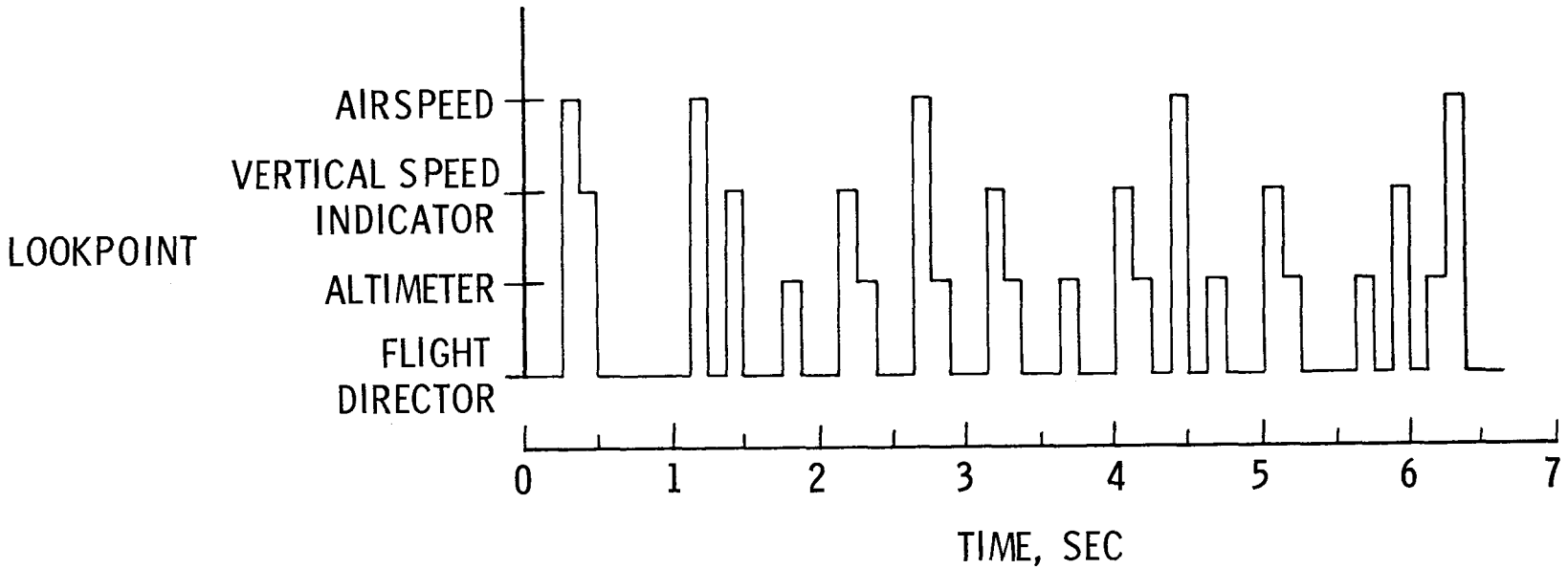

Figure 10.- Time history of lookpoints predicted by model for "coupled" landing approach.

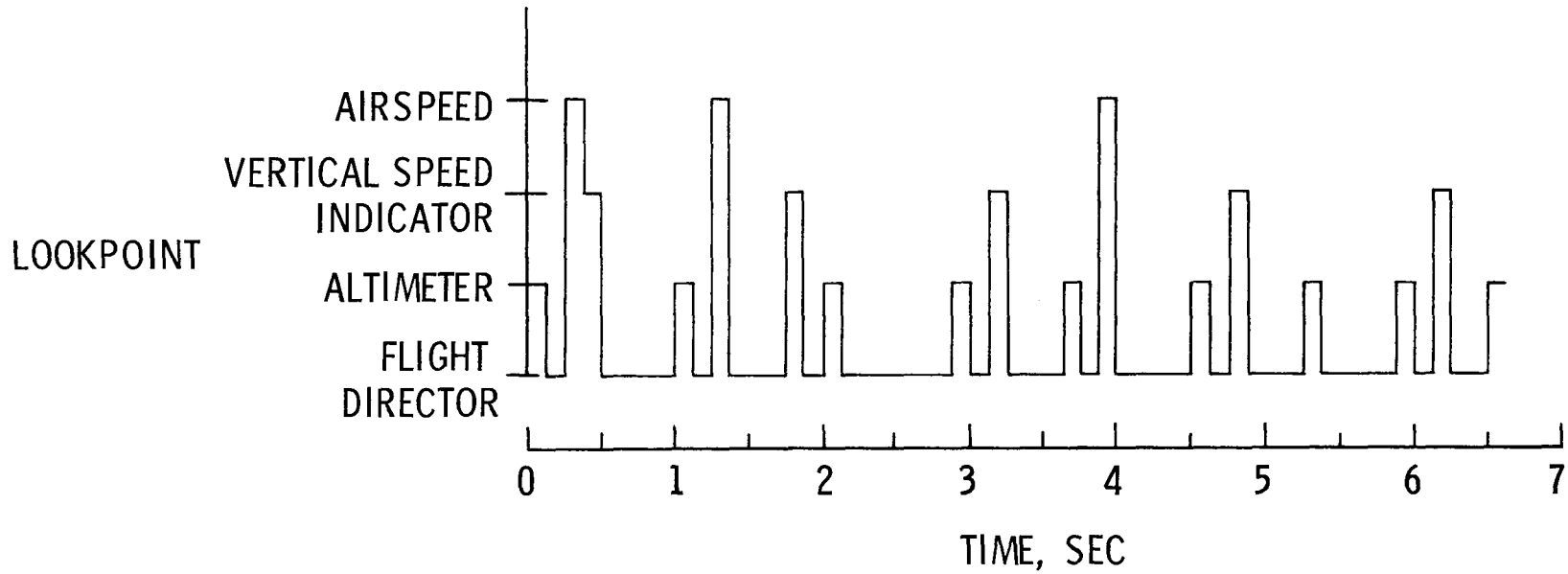

Figure 11.- Time history of lookpoints predicted by model for manual landing approach.